INTERNATIONAL JOURNAL OF AUTOMOTIVE AND MECHANICAL ENGINEERING (IJAME)
ISSN: 2229-8649 e-ISSN: 2180-1606
VOL. 19, ISSUE 4, 2022, 10121 – 10131
DOI: https://doi.org/10.15282/ijame.19.4.2022.09.0783

ORIGINAL ARTICLE

Effects of Solutionizing and Aging Alteration on Tensile Behavior of Stir Cast LM4-Si_3N_4 Composites

D. Srinivas, G. Shankar*, S. Sharma, A. Kini and M. Shettar

Department of Mechanical and Industrial Engineering, Manipal Institute of Technology, Manipal Academy of Higher Education, Manipal-576104, Karnataka, India

ABSTRACT – The main concern of this research is to identify the effect of multistage solutionizing and artificial aging behaviour on tensile behavior of LM4 + Si3N4 (1, 2, and 3 wt.%) composites. A two-stage stir casting method was employed to produce composites, which minimized the necessity for a lengthy and high-temperature preheating treatment of reinforcement and resulted in homogeneous reinforcement distribution. Cast composites were subjected to single-stage and multistage solutionizing heat treatment (SSHT and MSHT) followed by aging at 100 and 200°C. Peak hardness of the LM4 and cast composites was noted during artificial aging. With the increase in wt.% of reinforcement, the hardness of the composites increased. Cast composites subjected to MSHT and aging at 100°C displayed maximum hardness when matched to other combinations. Compared to as-cast LM4 hardness (70 VHN), L3SN (with MSHT + aged at 100°C) composite attained 124% higher hardness (157 VHN). UTS values followed a similar trend, compared to as-cast LM4 UTS (149 MPa), L3SN (with MSHT + aged at 100°C) composite attained 54% higher UTS (230 MPa). Major reasons for the improvement in mechanical properties of heat-treated composites are due to the existence of hard Si3N4 particles and the formation of θ'-Al2Cu and θ"-Al3Cu (metastable) phases. From the fracture surface analysis of LM4 and L3SN composite, it was concluded that the type of fracture experienced by LM4 is of ductile nature and that of the composite is of mixed nature.

ARTICLE HISTORY
Received: 17th Apr. 2022
Revised: 3rd Oct. 2022
Accepted: 21st Dec. 2022
Published: 28th Dec. 2022

KEYWORDS
Multistage solution heat treatment (MSHT);
Aging treatment;
Hardness;
Ultimate tensile strength;
Single-stage solution heat treatment (SSHT)

INTRODUCTION

Weight reduction and material performance enhancement have become essential objectives in many industries, including automotive, defence, and aerospace. Aluminum, which is abundant on earth and has a lower density than other popular materials (steel), is chosen to fill those gaps in industries [1]. Aluminum metal matrix composites (AMCs), which are lightweight and nonferrous alloy-based composites, have been popular in recent years due to their unique and highly valued features that may meet the needs of the industry [2], [3]. Our work focuses on LM4 (Al-Si hypoeutectic) alloy because of its low melting point and other decent mechanical properties, as well as its ability to retain tensile strength up to 200°C operating temperature [4]. The mechanical properties of this alloy can be improved by adding reinforcements such as TiB_2, B_4C, and Al_2O_3 [5]–[8]. We chose Si_3N_4 as a ceramic reinforcement for the composites fabrication in our study because it offers a favorable combination of physical and mechanical properties. Si_3N_4 is a non-oxide ceramic powder with a high melting point, hardness, and comparatively low density, making it a superior reinforcement for Al alloys. Si_3N_4 is commonly used in the preparation of rotors and bearings [9]. Several researchers have worked with Si_3N_4 as a reinforcing material for aluminum alloys, with some of the cases discussed below and illustrated in Table 1.

Ahmad et al. [10] studied the density variation in LM25 (2.69 g/cm^3)+Si_3N_4 (3.28 g/cm^3) composites. From the result, they concluded that there is a very minimal effect of Si_3N_4 on the density variation in composites. It varied between 2.68 to 2.738 g/cm^3 for 0 to 12 wt.% addition; this small variation is due to the density difference between reinforcement and base alloy. Alam et al. [11] mixed Si_3N_4 with Al powder to improve the wettability of the reinforcement with A356 and also confirmed that the presence of hard Si_3N_4 is responsible for the improvement in hardness and tensile strength. Similarly, Manjunath et al. [12] confirmed the improvement in mechanical properties of AA2219 after the addition of Si_3N_4 reinforcement when preheated at 670°C to improve the wettability. Mohanavel et al. [13] reported in their work that the grain alteration caused by Si_3N_4 to the alloy (AA7178) is one of the major reasons for the mechanical property improvement in composites. Table 1 shows the various fabrication processes employed by various researchers in the preparation of AMCs with Si_3N_4 as reinforcement. Different heat treatments are used to improve the mechanical properties of composites [14]. The most often used treatment for aluminum alloys is solutionizing and artificial aging. Xiu et al. [15] prepared Si_3N_4/Al composites using the pressure infiltration method; they observed that the bending strength of the prepared composites reduced as the vol.% of Si_3N_4 increased, but the properties can be greatly improved by T6 heat treatment. Zhigang et al. [16] prepared Al6061+Si_3N_4 composites by using sintering and hot extrusion process and studied the effect of Si_3N_4 on the artificial aging behaviour of prepared composites. It was concluded that there is no change in the grain structure of alloy and composite after solutionizing, and two-step aging resulted in an improvement

*CORRESPONDING AUTHOR | Gowrishankar | ✉ gowri.shankarmc@manipal.edu

of mechanical properties because of the ß" phase formed. The reinforcement addition has accelerated the aging kinetics. Zhang et al. [17] prepared Al+Si_3N_4 composites using the hot pressing method and from the tensile testing results, they concluded that the addition of Si_3N_4 caused improvement in UTS values and could maintain the ductility as well. As the Si_3N_4 vol.% increased, the fracture mechanism shifted from ductile to a mix of ductile and brittle fracture.

According to the literature review, there has been a lot of research done on ceramic powders as reinforcements, but we noticed a bit of a lag in the research involving Si_3N_4 as reinforcement for LM4 alloy as well as precipitation hardening treatment for the composites generated. To achieve uniform distribution after casting, many researchers have preheated the reinforcement powder at higher temperatures for a longer duration [12], [13], [15]. To avoid this, we used a two-stage stir casting in which we preheated the reinforcement at a lower temperature, added it to the semi-solid melt, and stirred for 5 minutes for better distribution. As indicated in Table 1, only a few researchers have performed heat treatment and researched the behaviour of composites, and the relevance of solutionizing and aging at different temperatures for different periods has not been explored. As a result, we concentrated our research on the fabrication of LM4+Si_3N_4 composites using a two-stage stir casting technique and subjecting them to SSHT and MSHT followed by artificial aging at 100 and 200°C. The hardness and tensile strength of heat-treated composite specimens matched to as-cast alloy. Microstructural and XRD analyses were carried out to validate the uniform reinforcement distribution and to identify the metastable stable phases responsible for mechanical property improvement. Fracture surface analysis was done for both as-cast and heat-treated tensile specimens to analyze fracture behaviour.

Table 1. Type, preparation, and mechanical property data of various Al-Si_3N_4 composites

Matrix	Reinforcement and quantity	Method of preparation	Type of heat treatment	Improvement (%) in properties of composites when compared to the as-cast alloy		Reference
				Hardness	UTS	
Al7075	Si_3N_4 (0-8 wt.%)	Stir casting	/	20	/	[18]
AA7075	Si_3N_4 (0-12 wt.%)	Electromagnetic stir casting	T6 (SHT – 500°C/6 h; aging – 150°C/24 h)	26	24	[19]
Al6061	Si_3N_4 (6 wt.%)	Ball milling, vacuum hot pressing	SHT – 530°C/1 h; single aging – 175°C/0-72 h, two-step aging – 175°C, 200°C/4 h	14	/	[16]
Al powder	Si_3N_4 whiskers	Hot pressing	/	/	97	[17]
AA2219	Si_3N_4 (3, 6, and 9 wt.%)	Stir casting	/	44	10	[12]
Al powders	Si_3N_4 whiskers	Hot pressing and hot extrusion	/	112	122	[20]
A356	Si_3N_4 (1-5 wt.%)	Stir casting	/	100	59	[11]
AA6061-T6	Si_3N_4 (10, 20 wt.%)	Stir casting	/	117.8	55.8	[21]
Al7068	Si_3N_4 (3, 5 wt.%)	Stir casting	/	50.8	41.8	[22]
AlSi10Mg	Si_3N_4 (5, 10, and 15 vol.%)	Laser powder-bed-fusion	/	46 (15 vol.%)	12 (10 vol.%)	[23]
AA2219	Si_3N_4 (3, 6, and 9 wt.%)	Stir casting	/	50	10	[24]

METHODOLOGY

Materials

Figure 1 illustrates the methodology used in this study, with a thorough description of each step, starting from raw material to composites testing. For composite preparation, LM4 was used as a base or matrix material, and Si_3N_4 as reinforcement material. LM4 material possesses a density of 2.75 g/cm^3, available with a hardness of 66-80 VHN and the melting point of LM4 is 660°C. It has silicon (Si) and copper (Cu) as major alloying elements. The chemical composition of LM4 used in this study is shown in Table 2. The physical properties of Si_3N_4 are given in Table 3. Optical microscopy (OM), scanning electron microscopy (SEM), and energy dispersive x-ray analysis (EDAX) were performed on Si_3N_4 powder to verify uniform particle size and the presence of Si and N elements. SEM and EDAX of the powder are displayed

in Figure 2. From this figure, we can confirm that almost all the Si_3N_4 particles are of uniform size and do not have any impurities on them.

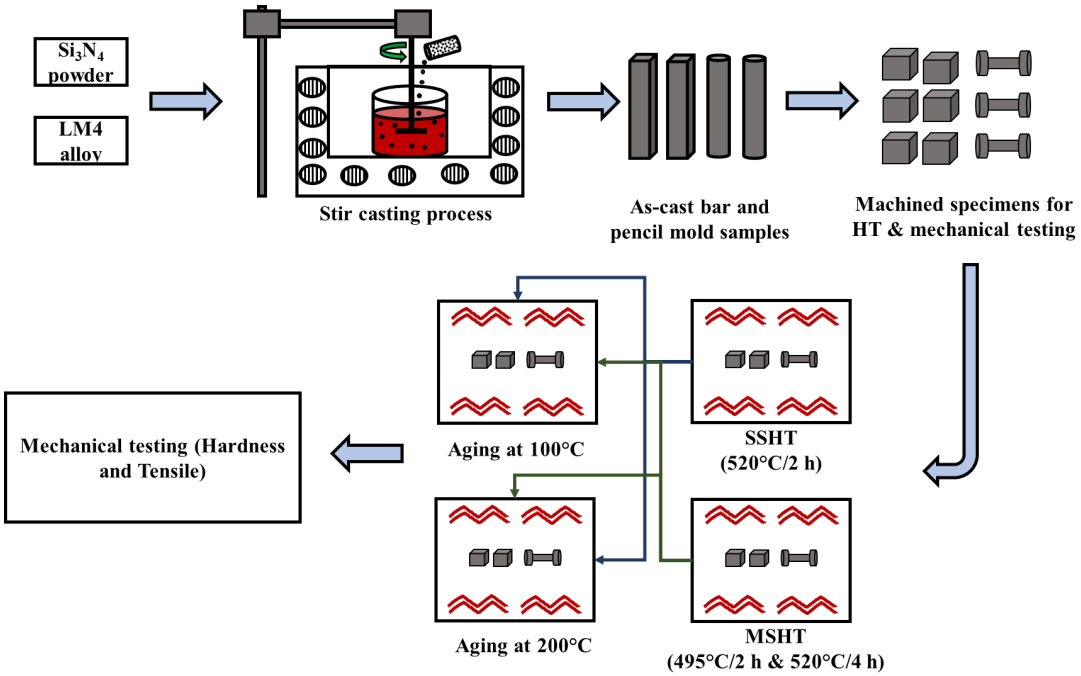

Figure 1. Methodology flow chart

Table 2. Chemical composition of LM4

Material	Sn	Fe	Ni	Mn	Cu	Ti	Mg	Si	Al
wt.%	0.045	0.641	0.03	0.121	2.476	0.045	0.176	5.925	Bal.

Table 3. Physical properties of Si_3N_4

Material appearance	Colour	Purity	Vickers hardness	Density	Average particle size	Melting point
Powder form	Light gray	99.9%	1835 VHN	3.17 g/cm^3	26 µm	1900 °C

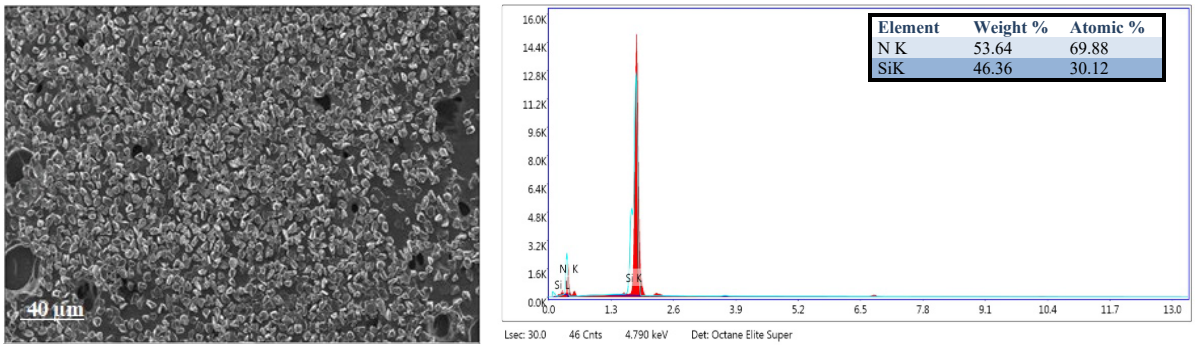

(a) (b)

Figure 2. (a) SEM micrograph and (b) EDAX of Si_3N_4 reinforcement powder

Composite Fabrication and Heat Treatment

The two-stage stir casting method (in Figure 3) used for the fabrication of composites is as follows; (i) 1600 grams of LM4 material was melted in a crucible at 780°C, (ii) Si_3N_4 reinforcement powder was preheated at 350°C/30 min before adding to LM4 melt [25], (iii) a mechanical stirrer was used to stir the LM4 melt until fine vortex formed and, proper stirring has to be performed to get uniform distribution of reinforcement in the matrix, (iv) after the clear formation of a vortex, preheated reinforcement was added gradually to molten slurry maintained at 600°C with the help of a spatula and stirred for about 5 min at 400 rpm, (v) then the temperature is raised to 730°C and stirring was continued for 10 min, (vi) after stirring, the molten mixture was poured into a preheated mold at 500°C/1 h and left for solidification. Cast bar and pencil molds are shown in Figure 3. During the casting of LM4+Si_3N_4 (1, 2, and 3 wt.%) composites, both stirring time and speed were kept constant. The casting of LM4+5 wt.% Si_3N_4 was also carried out. However, because the reinforcement particle size is extremely small, a great amount of powder was required to be added, the molten LM4 melt could not contain much of the powder, and it began to pop out; poor wettability might have been one of the reasons. Figure 4 depicts the reinforcement popup as well as the solidified picture of the cast composite that was poured into the

preheated mold. Later LM4+5 wt.% Si_3N_4 composites were successfully fabricated by increasing the preheating temperature of Si_3N_4 to 670°C for 15 min [12]. Increasing the preheating temperature allowed proper mixing of Si_3N_4 in the LM4 melt without popping out. The labeling for the cast composites is shown in Table 4.

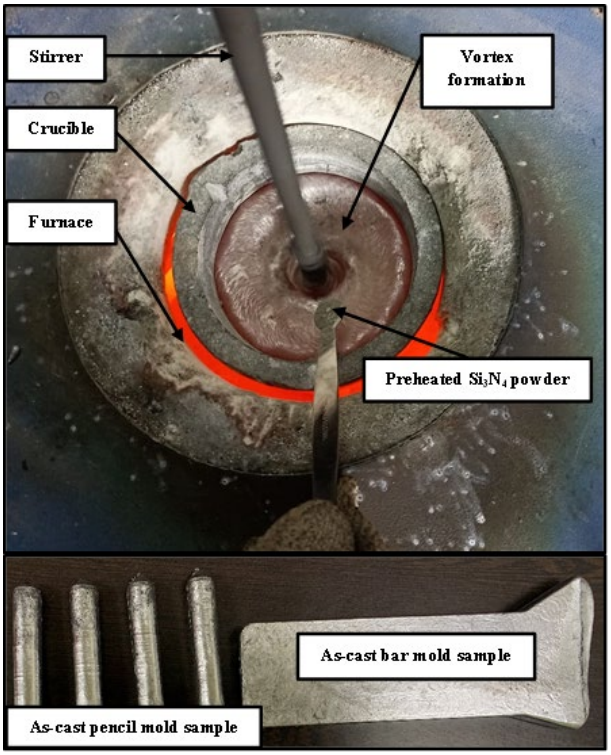

Figure 3. Stir casting process and cast samples

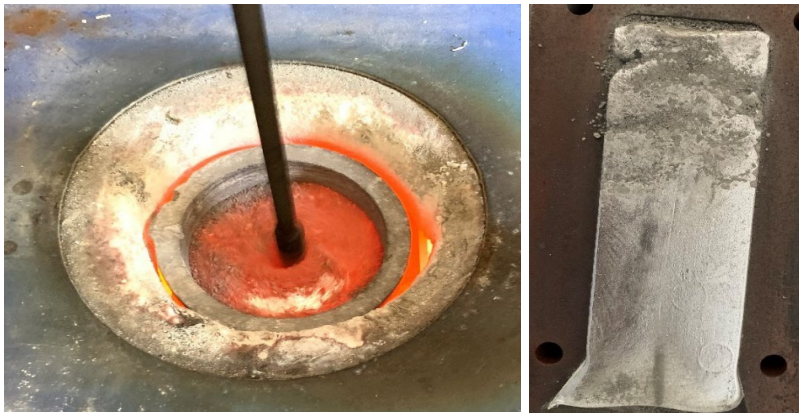

Figure 4. Reinforcement popup and solidified cast sample of failed L5SN composite

Table 4. Fabricated composites and their labeling

Base material	Reinforcement (wt.%)	Long name	Composite abbreviation
LM4	Si_3N_4 (1)	LM4 + 1 wt.% Si_3N_4	L1SN
LM4	Si_3N_4 (2)	LM4 + 2 wt.% Si_3N_4	L2SN
LM4	Si_3N_4 (3)	LM4 + 3 wt.% Si_3N_4	L3SN
LM4	Si_3N_4 (5)	LM4 + 5 wt.% Si_3N_4	L5SN

Cast samples were machined for further analysis and precipitation hardening process. Bar mold samples were machined into tiny cubes and were used for hardness testing, and pencil mold samples were machined as per ASTM-E8M standards to perform tensile tests. Figure 5 shows the images of machined specimens. During precipitation hardening treatment, two sets of specimens from each composite were subjected to MSHT and SSHT. The heating temperature and duration of both MSHT and SSHT were followed, as shown in figure 1. After solutionizing, specimens were quenched in hot water of 60°C to reduce the internal thermal stresses [26]. Quenched specimens were subjected to aging at 100 and 200°C at a different duration from 0 to 18 h. Samples were collected every 30 min and subjected to hardness testing until peak hardness was attained.

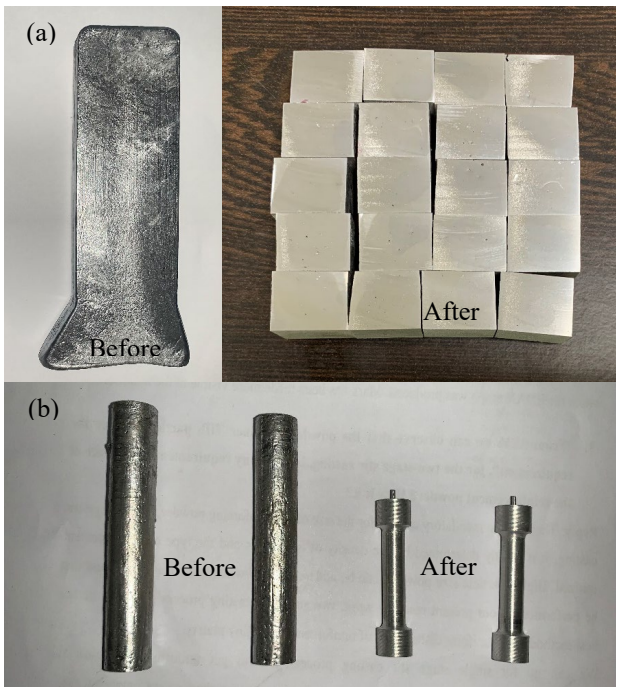

Figure 5. Machined as-cast composite specimens for hardness and tensile tests

Hardness and Tensile Test

Hardness tests were carried out using a Model - MMT X 7A-Micro Vickers Hardness Tester, with 200 gmf load and 15 seconds dwell time. Specimens were mirror polished before hardness testing using an automated disc polishing machine [METKON – FORCIPOL 102 with automated liquid dispenser – DOSIMAT 102] to remove impurities and oxides formed during heat treatment. Specimens used for microstructural analysis were also mirror-polished using the same polishing machine. Tensile testing was carried out with a PC-2000/605/06 Electronic Tensometer. The load was kept constant at 20 kN in break test mode while the test speed was maintained at 1 mm/min. Tensile tests were performed on both as-cast and peak-aged samples of LM4 and its composites.

RESULTS AND DISCUSSION

Microstructural Analysis

The key aspect in preparing composites is obtaining a homogeneous distribution of reinforcements in the matrix, as a homogeneous distribution of reinforcements can provide excellent mechanical properties to the produced composites. This procedure must be carried out correctly to avoid reinforcement particle segregation during pouring and solidification. OM and SEM analyses of L1SN, L2SN, and L3SN were carried out to confirm the uniform distribution of Si_3N_4 within the matrix. Figure 6(a) shows the OM image of L3SN composite, and 6(b) and 6(c) shows the SEM and EDAX analysis of L3SN composite specimen. From figure 6 (a) and 6(b), we can observe that the dark and bright spots, which are confirmed as Si_3N_4 particles by EDAX are distributed equally throughout the area. Even though there is a density difference between matrix and reinforcement clusters was not observed. Preheating of Si_3N_4 powder at 350 °C/30 min, stirring rpm of 400, and stirring time of nearly 20 min helped in attaining homogenous distribution of reinforcement within the matrix without any agglomeration and burnouts. Bonding between LM4 and Si_3N_4 turned out to be proper without any interface reactions. OM and SEM images below indicate that the composites were produced with low porosity, no agglomeration, and no air pockets; this was only possible because of the two-stage stir casting method's adequate stirring parameters.

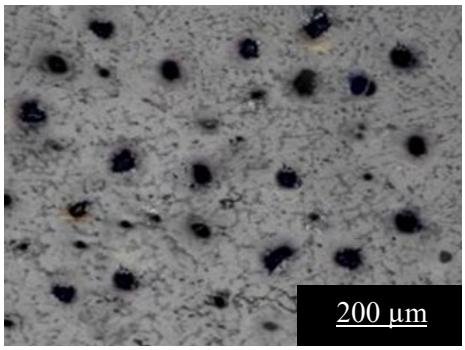

(a)

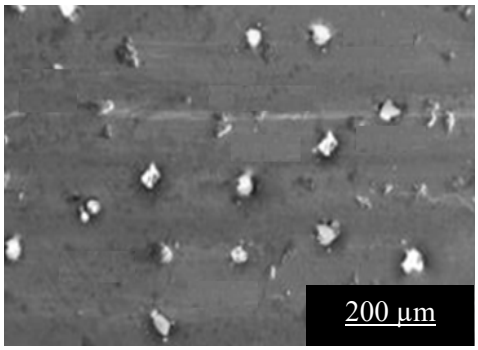

(b)

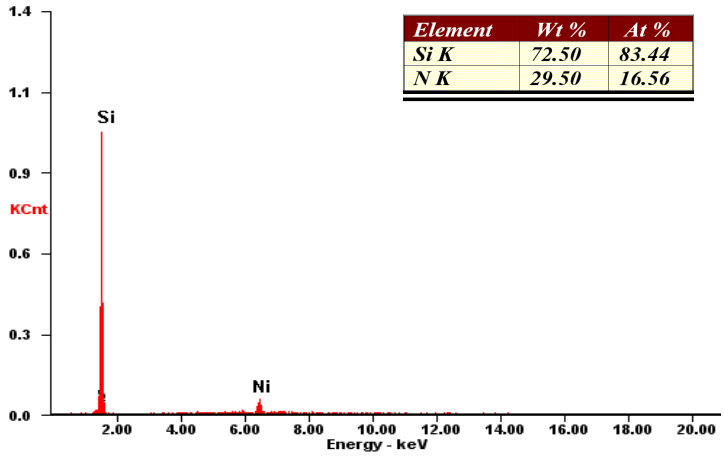

(c)

Figure 6. (a) Optical microscope image, (b) SEM micrograph and (c) EDAX of L3SN composite

Figure 7 shows the optical microscope image of the L5SN composite; from this image, we can see that particle agglomeration occurred. This might be due to poor wettability and high surface areas of reinforcement particles in the molten LM4 melt [27]. So, we restricted our study to only 3 wt.% of Si_3N_4 addition. All composite microstructures of L1SN, L2SN, and L3SN comprise a solid solution of LM4 with an inter-dendritic network of aluminum Si_3N_4 eutectic. Si_3N_4 particles serve as a nucleus around which the α-Al grains form during solidification.

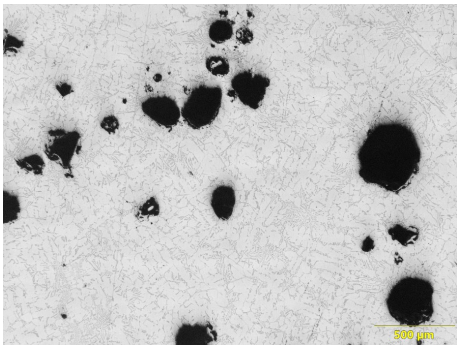

Figure 7. OM image of L5SN composite

Hardness Analysis

The hardness test was performed on LM4, L1SN, L2SN, and L3SN composite specimens in both as-cast condition and heat-treated (SSHT, MSHT followed by aging at 100 and 200°C) conditions. Figure 8 (a) to 8(d) show aging curves of alloy and its composites while Figure 9 shows the peak hardness comparison of alloy and its composites. The as-cast hardness of LM4, L1SN, L2SN, and L3SN are 70, 87, 88, and 90, respectively. With an increase in wt.% of reinforcement, there is an increase in hardness values, and as-cast L3SN displayed a 28.5% increase in hardness when compared to as-cast LM4. This improvement in hardness is due to the inclusion of hard ceramic particles into the matrix as well as good bonding between the matrix and reinforcement [28]. The hardness values right after SSHT and MSHT at 0 h of aging experience a drop in hardness values when compared to as-cast hardness values in Figure 8(a) to 8(d). During the solutionizing procedure, all solute-rich intermetallic phases combine with the matrix alloy and generate a homogeneous solid solution. A supersaturated solid solution is formed during the quenching process from higher to lower temperatures. It is a soft phase with good formability; however, it is volatile at room temperature. As a result, solutionized specimens exhibit lower hardness than as-cast specimens in both situations (SSHT and MSHT) [29]. These unstable phases strive to become stable secondary solute-rich phases along and inside grain boundaries [30], [31]. Hardness values of SSHT and MSHT cast composites gradually increased with aging time till peak age was attained. After the hardness values dropped, this phenomenon can be explained using the aging behaviour of materials [32], [33]. With an increase in wt.% of reinforcement, the time taken to reach peak hardness is reduced. Composites with MSHT + aging displayed higher hardness (37% higher) when compared to composites with SSHT + aging, this increase in hardness is because of a greater number of precipitates in MSHT samples than in SSHT samples [34]. Composites aged at 100°C demonstrated greater hardness than composites aged at 200°C; nevertheless, the time required to attain peak hardness for composites aged at 100°C is longer than for composites aged at 200°C. Figure 8 (a) to 8(d) show that the hardest materials were LM4, L1SN, L2SN, and L3SN after MSHT + aging at 100°C. When compared to as-cast LM4, its composites with MSHT + aging at 100°C improved by 93, 104, and up to 124% as in Figure 9.

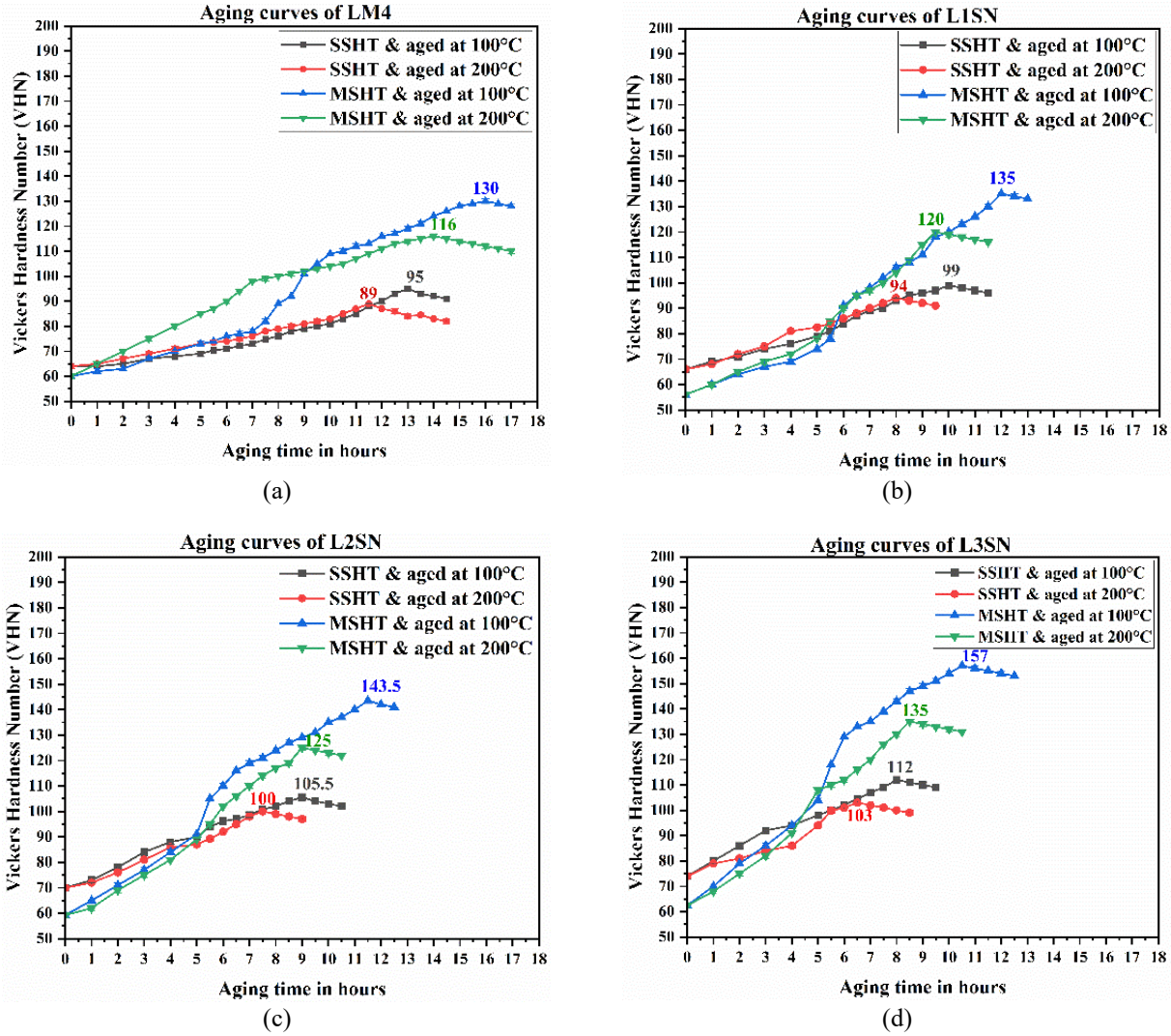

Figure 8. Aging curves of (a) LM4, (b) L1SN, (c) L2SN, and (d) L3SN during hardness measurement

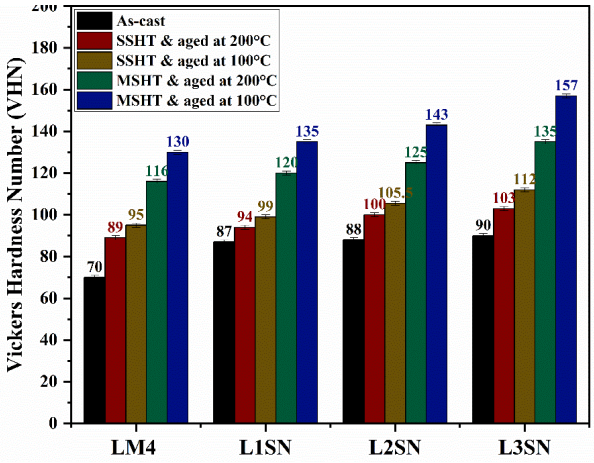

Figure 9. Peak hardness comparison of LM4, L1SN, L2SN, and L3SN

Tensile Strength Analysis

Tensile tests were carried out for as-cast and peak-aged (MSHT + aged at 100°C) composites. From Figure 10, we can see that with an increase in wt.% of the reinforcement, the UTS values of as-cast composites increased. The improvement in UTS values is because of the addition of hard Si3N4 to the soft LM4 matrix; this increased the resistance to deformation by creating a blockage to the dislocation motion. The thermal mismatch between Si_3N_4 (1.4-3.7×10^{-6}/K) and LM4 (24×10^{-6}/K) caused an increment of dislocation density and load-bearing capacity, which in turn improved tensile strength. Hard Si_3N_4 particles provide more heterogenous nucleation sites during solidification, which reduces the grain size of aluminum alloy [21]. MSHT and artificial aging caused the formation of metastable phases, and all these microstructural changes together resist the deformation forces during testing, which improved the UTS and hardness

properties. Compared to LM4 (as-cast), composites (as-cast) displayed 10, 22, with up to 32% improvement in UTS values, whereas peak aged (MSHT + aging at 100°C) composites displayed 38, 46, with up to 54% improvement.

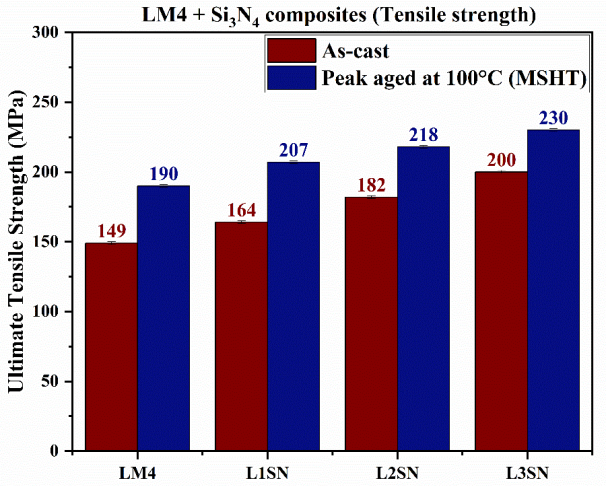

Figure 10. UTS values of LM4, L1SN, L2SN, and L3SN in as-cast and peak aged at 100°C (MSHT)

XRD Analysis

Another reason for the improvement in mechanical properties of composites is due to the modification in microstructure that occurred during heat treatment [35]. XRD of the L3SN composite is shown in Figure 11. θ'-Al_2Cu and θ"-Al_3Cu are the metastable phase that are major contributors to the improvement in hardness of the heat-treated composites [36], [37]. As composites subjected to MSHT possess a greater number of precipitates, they tend to precipitate and form intermetallic phases, hence higher hardness values.

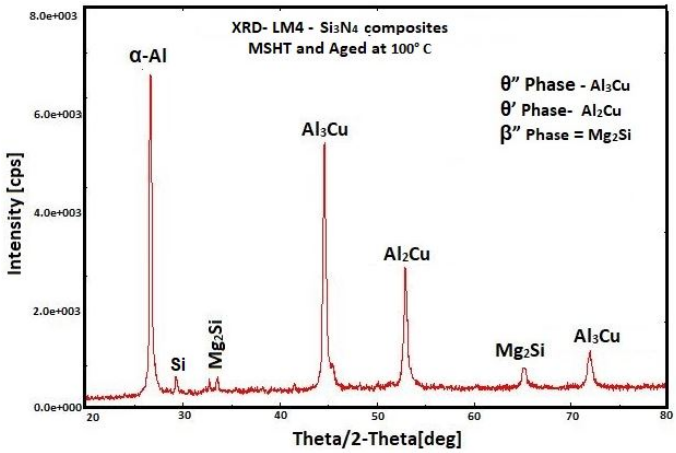

Figure 11. XRD of L3SN (MSHT + aged at 100°C) composite

Fracture Surface Analysis

Fracture analysis of LM4 and L3SN composite (both as-cast and peak aged) were done after the tensile test. Figure 12(a) and 12(b) shows the fracture surface of as-cast LM4, and 12(c) and 12(d) show the fracture surface of peak aged (MSHT + aged at 100°C) LM4. Similarly, Figure 13(a) and 13(b) show the fracture surface of the as-cast L3SN composite, and 13(c) and 13(d) show the fracture surface of peak aged (MSHT + aged at 100°C) L3SN composite. Figure 12 (a) and 12(b) of the as-cast LM4 fracture surface clearly show that it experienced plastic flow during the tensile test, which indicates the ductile type of fracture and mode of failure is dimple rupture. This ductile void progression is because of the buildup of both micro and macro voids of various shapes that are randomly dispersed in the specimen. When it comes to Figures 12(c) and 12(d), we can see a mixed mode of failure, and more flat surfaces can be seen, which resulted partly in brittle failure.

In L3SN of Figures 13(a) and 13(b), the size of dimples formed is small when compared to the alloy, and the surface flatness is more. This explains that the type of fracture in composites is more of a brittle nature than ductile. This is because of the reduction in grain size, which restricts the dislocation movement. The addition of Si_3N_4 reduced the proportion of dimples, so the mode of failure steadily switched from ductile to brittle. A major part of the fracture observed is flat and brittle type, and some reasonable portion seemed to have experienced ductile fracture [13]. Figure 13(a) and 13(b) demonstrate a large number of broken reinforcement phases in the fractured area, indicating that the bond between reinforcement and matrix is strong [24]. Tough interface bonding is capable of successfully transferring loads, preventing crack propagation, and strengthening composite materials [23]. As the wt.% of Si_3N_4 increases, the composites experience

more brittle failure and less ductile failure. In Figure 13(c) and 13(d), we can see the increase in the flatness of the surface, and this explains the brittle failure of the peak aged composite, the presence of metastable phases, and a drastic reduction in the size of dimples are also the reasons behind brittle failure [12]. Figure 13(e) shows the EDAX of the L3SN (MSHT + aged at 100°C) composite fracture surface, which confirmed the presence of Si and N in it.

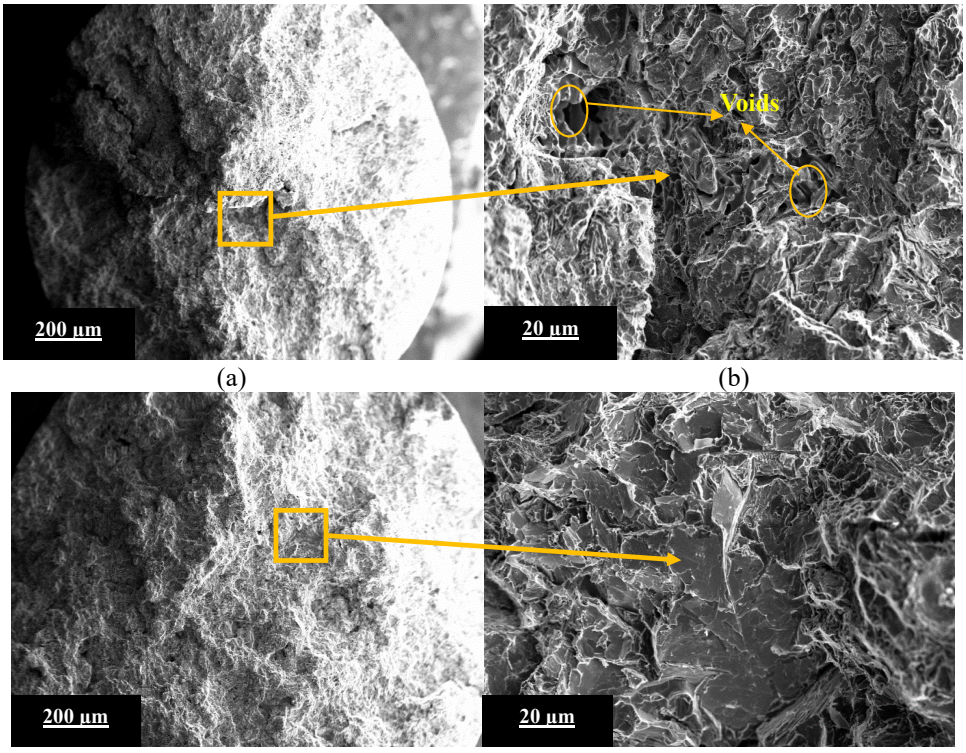

Figure 12. (a),(b) Fracture surface of as-cast LM4, and (c),(d) fracture surface of peak aged (MSHT + aged at 100°C) LM4

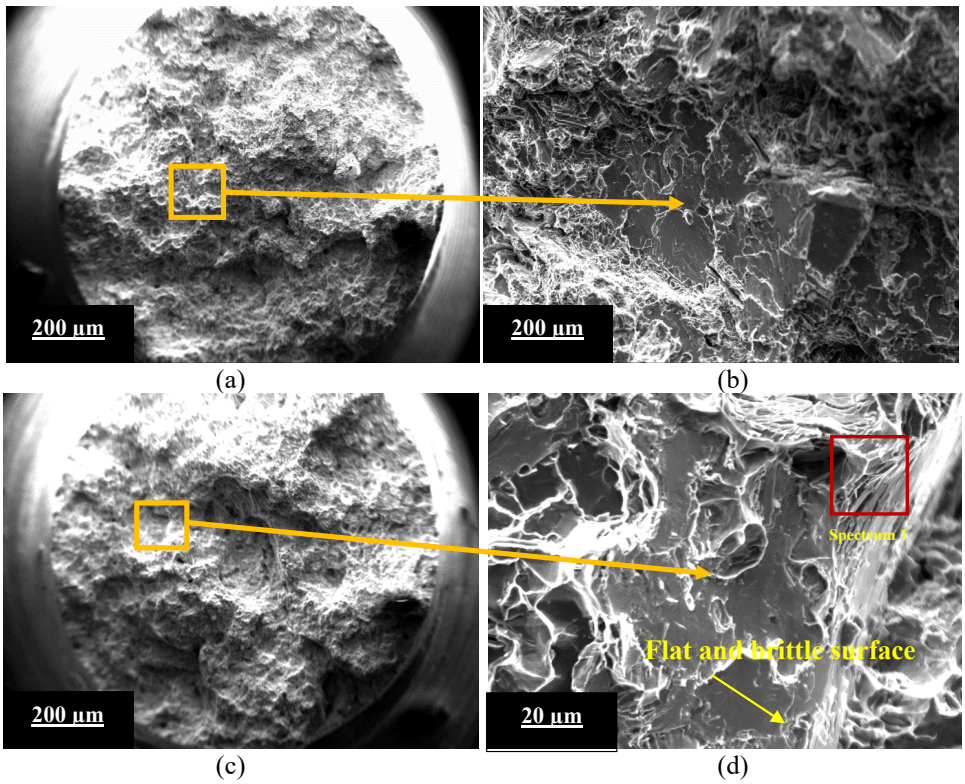

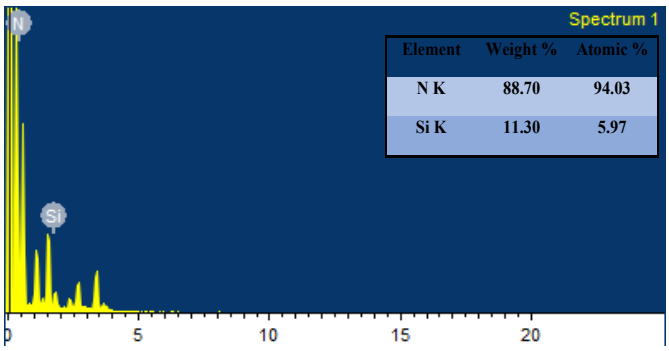

(e)

Figure 13. (a), (b) Fracture surface of as-cast L3SN, (c), (d) fracture surface of peak aged (MSHT + aged at 100°C) L3SN, and (e) EDAX of L3SN (MSHT + aged at 100°C) composite

CONCLUSIONS

The following conclusions were drawn from the results obtained:

i. Casting parameters used in the two-stage stir casting process were found to be efficient in producing fine composites with uniform reinforcement distribution and zero flaws, as validated by SEM and EDAX analysis.
ii. An increase in wt.% of the reinforcement increased the hardness properties by 24-28% and tensile by 10-34% of as-cast composites when matched to as-cast LM4.
iii. Among various precipitation hardening treatments carried out (SSHT, MSHT followed by artificial aging at 100 and 200°C), MSHT + aging at 100°C produced the highest hardness and tensile values.
iv. Compared to as-cast LM4, MSHT + aged at 100°C composite samples displayed 92-124% and 38-54% improvement in hardness and tensile values, respectively.
v. XRD analysis confirmed the formation of Al_2Cu and Al_3Cu metastable phases in the L3SN (MSHT + aged at 100°C) composite specimen that is responsible for the improvement in mechanical properties.
vi. Fracture surface analysis of LM4 confirmed the ductile nature of the fracture, whereas in composites (as-cast and heat-treated), a mixed mode of fracture is evident, with the majority of it being brittle.

ACKNOWLEDGEMENT

No funding agencies have funded this work.

REFERENCES

[1] Y. Mazaheri, F. Karimzadeh, and M. H. Enayati, "A novel technique for development of A356/Al_2O_3 surface nanocomposite by friction stir processing," *Journal of Materials Processing Technology*, vol. 211, no. 10, pp. 1614–1619, 2011.
[2] M. A. Abdelgnei, M. Z. Omar, M. J. Ghazali, M. N. Mohammed, and B. Rashid, "Dry sliding wear behaviour of thixoformed Al-5.7Si–2Cu-0.3 Mg alloys at high temperatures using taguchi method," *Wear*, vol. 442–443, p. 203134, 2020.
[3] V. Subravel, T. Padmanaban, T. V. Rajamurugan, and M. Seeman., "The effect of GTAW variants on tensile and microstructural properties of AZ31B magnesium alloy joints," *Advances in Materials Science and Engineering*, vol. 2022, pp. 1–8, Oct. 2022.
[4] Barron-Clark castings ltd, "LM4 aluminium casting alloy," *Hall Botterill*, no. M, pp. 2–5, [Online]. Available: https://www.barronclark-castings.co.uk/alloy-range/ [Accessed: April 15, 2022]
[5] M. O. Shabani, A. Mazahery, M. R. Rahimipour, and M. Razavi, "FEM and ANN investigation of A356 composites reinforced with B_4C particulates," *Journal of King Saud University - Engineering Sciences*, vol. 24, no. 2, pp. 107–113, 2012.
[6] S. Poria, P. Sahoo, and G. Sutradhar, "Tribological characterization of stir-cast aluminium-TiB_2 metal matrix composites," *Silicon*, vol. 8, no. 4, pp. 591–599, 2016.
[7] R. Shu, X. Jiang, J. Li, Z. Shao, D. Zhu, and T. Song, "Microstructures and mechanical properties of Al-Si alloy nanocomposites hybrid reinforced with nano-carbon and in-situ Al_2O_3," *Journal of Alloys and Compounds*, vol. 800, pp. 150–162, 2019.
[8] S. Prakash, C. S. Abdul Favas, I. Ameeth Basha, R. Venkatesh, and M. Prabhahar, "Investigation of mechanical and tribological characteristics of medical grade Ti6al4v titanium alloy in addition with corrosion study for wire EDM process," *Advances in Materials Science and Engineering*, vol. 2022, pp. 1–10, Sep. 2022.
[9] C. Zhang, D. Yao, J. Yin, K. Zuo, and Y. Xia, "Effects of ß-Si_3N_4 whiskers addition on mechanical properties and tribological behaviors of Al matrix composites," *Wear*, vol. 430–431, no. February, pp. 145–156, 2019.
[10] Z. Ahmad, S. Khan, and S. Hasan, "Microstructural characterization and evaluation of mechanical properties of silicon nitride reinforced LM25 composite," *Journal of Materials Research and Technology*, vol. 9, no. 4, pp. 9129–9135, 2020.
[11] M. T. Alam, M. Azhar, and Y. Rafat, "Physical, mechanical and morphological characterization of A356/Si_3N_4 nanoparticles stir casting composites," *Journal of Engineering Research*, pp. 1–16, 2022.
[12] C. J. Manjunatha, V. Narayana, and D. B. P. Raja, "Investigating the effect of Si_3N_4 reinforcement on the morphological and mechanical behavior of AA2219 alloy," *Silicon*, vol. 14, no. 6, pp. 2655–2667, 2022.
[13] V. Mohanavel and M. Ravichandran, "Optimization of parameters to improve the properties of AA7178/Si_3N_4 composites employing taguchi approach," *Silicon*, vol. 14, no. 4, pp. 1381–1394, 2022.
[14] T. Ramkumar, A. Haiter Lenin, M. Selva kumar, M. Mohanraj, S. C. Ezhil Singh, and M. Muruganandam, "Influence of rotation speeds on microstructure and mechanical properties of welded joints of friction stir welded AA2014-T6/AA6061-T6

alloys," *Proceedings of the Institution of Mechanical Engineers, Part E: Journal of Process Mechanical Engineering*, vol.1, p. 095440892210776, Mar. 2022.

[15] Z. Y. Xiu, G. Q. Chen, G. H. Wu, W. S. Yang, and Y. M. Liu, "Effect of volume fraction on microstructure and mechanical properties of Si_3N_4/Al composites," *Trans. Nonferrous Met. Soc. China (English Ed.)*, vol. 21, no. SUPPL. 2, pp. s285–s289, 2011.

[16] Z. Li, L. Chen, B. Que, G. Zhao, and C. Zhang, "Effects of artificial aging on precipitation behavior, mechanical properties and corrosion resistance of Si_3N_4/6061Al composite fabricated by sintering and hot extrusion processes," *Journal of Materials Processing Technology*, vol. 306, no. March, p. 117644, 2022.

[17] C. Zhang, J. Yin, D. Yao, K. Zuo, Y. Xia, and H. Liang, "Enhanced tensile properties of Al matrix composites reinforced with β-Si_3N_4 whiskers," *Composites Part A: Applied Science and Manufacturing*, vol. 102, pp. 145–153, 2017.

[18] M. I. Ul Haq and A. Anand, "Dry sliding friction and wear behavior of AA7075-Si_3N_4 composite," *Silicon*, vol. 10, no. 5, pp. 1819–1829, 2018.

[19] J. M. Mistry and P. P. Gohil, "Experimental investigations on wear and friction behaviour of Si_3N_{4p} reinforced heat-treated aluminium matrix composites produced using electromagnetic stir casting process," *Composites Part B: Engineering,* vol. 161, no. August 2018, pp. 190–204, 2019.

[20] C. Zhang, Y. P. Zeng, D. Yao, J. Yin, K. Zuo, and Y. Xia, "The improved mechanical properties of Al matrix composites reinforced with oriented β-Si_3N_4 whisker," *Journal of Materials Science & Technology.*, vol. 35, no. 7, pp. 1345–1353, 2019.

[21] B. A. Kumar, M. M. Krishnan, A. F. Sahayaraj, M. R. A. Refaai, G. Yuvaraj, and D. Madhesh, "Characterization of the aluminium matrix composite reinforced with silicon nitride (AA6061/Si_3N_4) synthesized by the stir casting route," *Advances in Materials Science and Engineering*, vol. 2022, pp. 1–8, Jan. 2022.

[22] T. Buddi and R. S. Rana, "Fabrication and finite element analysis of two wheeler connecting rod using reinforced aluminum matrix composites Al7068 and Si_3N_4," *Materials Today Proceeding*, vol. 44, pp. 2471–2477, 2021.

[23] K. Miao, H. Zhou, Y. Gao, X. Deng, Z. Lu, and D. Li, "Laser powder-bed-fusion of Si_3N_4 reinforced AlSi10Mg composites: Processing, mechanical properties and strengthening mechanisms," *Materials Science and Engineering: A*, vol. 825, no. August, p. 141874, 2021.

[24] C. J. Manjunatha, B. Venkata Narayana, D. Bino Prince Raja, and R. S. Rimal Isaac, "Tribological, thermal and corrosive behaviour of aluminium alloy 2219 reinforced by Si_3N_4 nanosized powder," *Silicon*, vol. 14, no. 8, pp. 4325–4336, 2022.

[25] G. B. V. Kumar, P. P. Panigrahy, S. Nithika, R. Pramod, and C. S. P. Rao, "Assessment of mechanical and tribological characteristics of silicon nitride reinforced aluminum metal matrix composites," *Composites Part B: Engineering*, vol. 175, no. June, p. 107138, 2019.

[26] V. R. Rajeev, D. K. Dwivedi, and S. C. Jain, "Dry reciprocating wear of Al-Si-SiC_p composites: A statistical analysis," *Tribology International*, vol. 43, no. 8, pp. 1532–1541, 2010.

[27] M. Karbalaei Akbari, O. Mirzaee, and H. R. Baharvandi, "Fabrication and study on mechanical properties and fracture behavior of nanometric Al_2O_3 particle-reinforced A356 composites focusing on the parameters of vortex method," *Materials & Design.*, vol. 46, pp. 199–205, 2013.

[28] M. Shettar, P. Hiremath, G. Shankar, A. Kini, and S. Sharma, "Tribolayer behaviour and wear of artificially aged Al6061 hybrid composites," *International Journal of Automotive and Mechanical Engineering*, vol. 18, no. 2, pp. 8668–8676, 2021.

[29] R. Rajesh, S. Sharma, and M. C. Gowrishankar, "Influence of solutionizing and aging treatments on mechanical behavior of stir-cast eutectoid steel powder reinforced Al 7075 metal matrix composites," *International Journal of Automotive and Mechanical Engineering*, vol. 15, no. 3, pp. 5583–5591, Oct. 2018.

[30] M. C. Gowrishankar, P. Hiremath, M. Shettar, S. Sharma, and S. Rao U, "Experimental validity on the casting characteristics of stir cast aluminium composites," *Journal of Materials Research and Technology.*, vol. 9, no. 3, pp. 3340–3347, May 2020.

[31] P. K. Jayashree, M. C. Gowrishankar, S. Sharma, R. Shetty, M. Shettar, and P. Hiremath, "Influence of homogenization and aging on tensile strength and fracture behavior of TIG welded Al6061-SiC composites," *Journal of Materials Research and Technology*, vol. 9, no. 3, pp. 3598–3613, 2020.

[32] D. K. B. Donald R Askeland, Pradeep P Fulay, *Essentials of materials science and engineering: SI edition*. 2nd ed., Noida: Cengage Learning, 2008.

[33] S. Sathyashankara, M. Guru, G. Shankar, A. Kini, M. Shettar, and P. Hiremath, "Aging kinetics and microstructural features of Al6061-SiC+B_4C stir cast hybrid composites," *International Journal of Automotive and Mechanical Engineering*, vol. 16, no. 4, pp. 7211–7224, Dec. 2019.

[34] Srinivas D., S. Sharma, M. C. Gowrishankar, P. Hiremath, and M. Shettar, "Effect of single and multistage solution heat treatment on age hardened A319 alloy," *AIP Conference Proceedings*, vol. 2421, no. 1, p. 040001, 2022.

[35] M. C. G. Shankar, J. P. K, S. S. Sharma, R. Shetty, and K. Vinay, "Quality enhancement of TIG welded Al6061 SiC_p composites by age hardening process," *International Journal of Automotive and Mechanical Engineering*, vol. 15, no. 3, pp. 5573–5582, Oct. 2018.

[36] H. M. Medrano-Prieto, C. G. Garay-Reyes, C. D. Gómez-Esparza, J. Aguilar-Santillán, M. C. Maldonado-Orozco, and R. Martínez-Sánchez, "Evolution of microstructure in Al-Si-Cu system modified with a transition element addition and its effect on hardness," *Materials Research*, vol. 19, pp. 59–66, 2016.

[37] J. Y. Hwang, R. Banerjee, H. W. Doty, and M. J. Kaufman, "The effect of Mg on the structure and properties of Type 319 aluminum casting alloys," *Acta Materialia*, vol. 57, no. 4, pp. 1308–1317, 2009.